

DEVELOPMENT OF WIND TURBINE CONTROL ALGORITHMS FOR INDUSTRIAL USE

T.G. van Engelen, E.L. van der Hooft, P. Schaak

Energy research Centre of the Netherlands (ECN), Wind Energy

P.O. Box 1, NL-1755 ZG Petten, The Netherlands

Telephone: ++31 224 564141

Telefax: ++31 224 568214

email: vanengelen@ecn.nl

ABSTRACT: A tool has been developed for design of industry-ready control algorithms. These pertain to the prevailing wind turbine type: variable speed, active pitch to vane. Main control objectives are rotor speed regulation, energy yield optimisation and structural fatigue reduction. These objectives are satisfied through individually tunable control loops. The split-up in loops for power control and damping of tower and drive-train resonance is allowed by the use of dedicated filters. Time domain simulation results from the design tool show high-performance power regulation by feedforward of the estimated wind speed and enhanced damping in sideward tower bending by generator torque control. The tool for control design has been validated through extensive test runs with the authorised aerodynamic code PHATAS-IV.

Keywords: Control, Variable speed operation, Dynamic models.

1. INTRODUCTION

The number of wind turbine manufacturers that apply pitch control towards feathering position for power limitation is increasing considerably. Usually, pitch-to-vane control is combined with variable speed operation, which is facilitated by commercially available fast switching components in power electronics. Operation outside stall conditions and enhanced energy yield around and below nominal wind speed are major drivers towards this concept. In comparison with power reduction by stall, the axial blade and tower loading is smaller and the aerodynamic behaviour is much better predictable. Especially at offshore siting the first feature is being considered more important than ever because of the extreme high reliability requirements.

This situation raises the need for control algorithms for variable speed pitch-to-vane wind turbines. For this reason, a design tool for such control algorithms has been developed at ECN [4]. This paper addresses the following topics of the *control tool*:

- problem identification and approach;
- turbine modelling and design principles;
- time domain simulation results.

2. CONTROL PROBLEM AND APPROACH

The main control loops concern the power production and rotor speed behaviour. Besides, control loops can be added for compensation of resonances (active damping). The latter loops are not allowed to significantly disturb the primary control functions. The resonances may appear in the rotor blades, the drive-train and the tower. In a multivariable design approach [1] the difference between all loops will not exist any more. In the developed design tool, the different control loops (fig. 1) are designed separately.

Separate loop design is enabled because the frequency ranges of the phenomena to be controlled significantly differ, which is illustrated in figure 1. The following typical frequencies exist:

- ω_{v_w} : rotor uniform turbulence (~ 0.07 Hz);
- ω_{0_t} : first tower bending mode (~ 0.35 Hz);
- ω_{0_d} : first shaft distortion mode (~ 2.5 Hz).

Aerodynamic and electric *power* control (thick-line blocks) concerns frequencies around ω_{v_w} . Tower bending and shaft

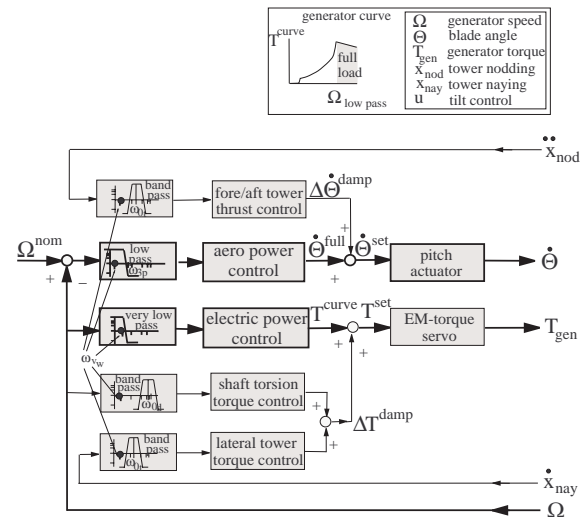


Figure 1: Feedback loops for control of rotor speed, power, tower bending and shaft distortion

distortion damping are typical narrow band processes around ω_{0_t} and ω_{0_d} , both (far) beyond ω_{v_w} (low- and band-pass filters in fig. 1). Furthermore, the frequency ω_{3p} applies ($\sim 0.6 - 1.2$ Hz). This is the center frequency of the effects of rotationally sampled turbulence and tower shadow. For a 3-bladed rotor, this is 3 times the rotational frequency (3p); for a 2-bladed rotor this ω_{2p} (2p), which does not differ much from ω_{3p} as the rotor speed is considerably higher for a 2-bladed. A suitable filter should eliminate these *Bp*-effects in the pitch-actuator activity ($B=2,3$). However, an exception can be made for the control loop on shaft distortion as this loop can also be used for reduction of inertia loads caused by '*Bp* rotor acceleration'.

The control scheme in fig. 1 does not deal with resonance of rotor blades because it is limited to *active* damping only. Blade resonance is usually reduced by *passive* damper devices ('mass spring damper' systems).

3. MODELLING AND CONTROL SYNTHESIS

The next subsections deal with the turbine model for control design and the synthesis principles of the identified loops.

3.1 Model for control design

The control tool includes models for wind and wave influences and for the dynamic response of the wind turbine. The model features are listed below and discussed afterwards.

External influences:

- stochastic wind and wave generation;
- aerodynamics by BEM-theory;
- dynamic inflow effect of blade pitching;
- hydrodynamics by Morison's equation.

Wind turbine system dynamics:

- first bending mode of tower (2 directions);
- first distortion mode of drive-train;
- linear servo behaviour for generator torque;
- non-linear servo behaviour for pitch actuation;
- delayed and quantized measurements.

The stochastic wind simulation is based on a rotor-wide description of the effect of rotationally sampled wind turbulence, tower shadow and wind shear. This approach is based on the modelling principle in [3]. A wind signal is obtained by inverse Fourier transform of 'the rotor-wide' power spectrum of the wind field as 'sampled' by the rotor blades. This spectrum is derived from auto power spectra and coherence functions in accordance with IEC standards. Figure 2 shows a typical generated wind speed signal; the detailed lower graph visualises the effect of rotational sampling and tower shadow on this signal (B_p -effects).

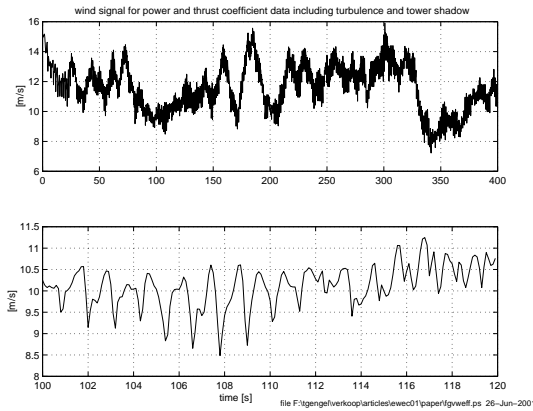


Figure 2: Realisation of rotor-wide wind speed

The rotor-wide wind speed V_w is fed through power and thrust coefficient data (C_p , C_t) for conversion to the aerodynamic torque T_a and axial force F_a (with nodding speed \dot{x}_{nd} ; rotor blade radius R_b , tip speed ratio λ):

$$\begin{aligned} T_a &= C_p(\theta^{ac}, \lambda) / \lambda \cdot \frac{1}{2} \rho \pi R_b^3 \cdot (V_w - \dot{x}_{nd})^2, \\ F_a &= C_t(\theta^{ac}, \lambda) \cdot \frac{1}{2} \rho \pi R_b^2 \cdot (V_w - \dot{x}_{nd})^2. \end{aligned}$$

The pitch angle value θ^{ac} as used in aerodynamic conversion is obtained from the 'physical' pitch angle value θ^{ph} by having θ^{ph} led through a so called lead-lag filter. This filter models the dynamic inflow effect of pitching through the following differential equation:

$$\tau_{DI} \cdot \frac{d}{dt} (\theta^{ac}) + \theta^{ac} = \tau_{dDI} \cdot \frac{d}{dt} (\theta^{ph}) + \theta^{ph}.$$

The time constants τ_{DI} and τ_{dDI} depend on the operating conditions. The actual values are obtained from polynomial

expressions in the pitch angle. The approach is based on the dynamic inflow modelling principle in [6].

The stochastic wave simulation is based on water depth dependent power spectra of the wave velocity and the wave acceleration. All these spectra are governed by the power spectrum of the surface elevation through the linear wave theory (Airy) [7]. Figure 3 shows for a water depth d of 20 m the (fully) correlated horizontal wave speed and acceleration signals on 55%, 65%, up to 95% of d above the sea bottom. A Pierson Moskowitz wave spectrum has been applied at an average wind speed of 12 m/s.

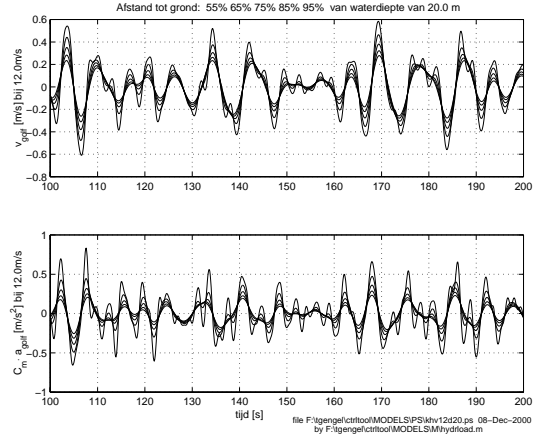


Figure 3: Realisation of wave speed and acceleration

Note that the lower graph in fig. 3 shows the product of mass coefficient C_m and wave acceleration a . This product is the 'force effective' acceleration with wave diffraction included as proposed by MacCamy and Fuchs [2]. If the waves are perpendicular to the wind, Morison's equation for the (lateral) wave force per unit tower length f_{hy_z} on z m below the sea surface is given by

$$\begin{aligned} f_{hy_z} &= \rho_{water} \cdot \frac{1}{4} \pi D_z^2 \cdot (\dot{w}_z^{eff} - \ddot{x}_{ny_z}) + \dots \\ C_d^H &\cdot \frac{1}{2} \rho_{water} \cdot D_z \cdot (w_z - \dot{x}_{ny_z}) \cdot |w_z - \dot{x}_{ny_z}|, \end{aligned}$$

with tower diameter D_z , wave speed w_z and force effective acceleration \dot{w}_z^{eff} , naying speed \dot{x}_{ny_z} and acceleration \ddot{x}_{ny_z} . Realistic values for the drag coefficient C_d^H lay between 0.6 and 1.2 [7].

Tower bending and drive-train dynamics are modelled by the following set of mutually dependent differential equations (waves perpendicular to wind):

$$\begin{aligned} m_t \ddot{x}_{nd} &= -k_t \dot{x}_{nd} - c_t x_{nd} + F_a \cos \theta_{tilt}, \\ m_t \ddot{x}_{ny} &= -k_t \dot{x}_{ny} - c_t x_{ny} + \frac{3}{2} \frac{T_{nac}}{L_t} + \dots \\ &\quad \int_0^d \mathcal{F}(f_{hy_z}) dz, \\ \frac{J_r \cdot J_g}{J_r + J_g} \cdot \dot{\gamma} &= -c_d \cdot \gamma - k_d \cdot \dot{\gamma} + \dots \\ &\quad \frac{J_g}{J_r + J_g} \cdot (T_a - T_\ell) + \frac{J_r}{J_r + J_g} \cdot T_e, \\ J_r \cdot \dot{\Omega}_r &= -c_d \cdot \gamma - k_d \cdot \dot{\gamma} + T_a - T_\ell. \end{aligned}$$

The shaft distortion speed $\dot{\gamma}$ is the difference between rotor speed Ω_r and 'slow shaft level' generator speed Ω_g / i_{gb} (gearbox transmission ratio i_{gb}). J_r and J_g are corresponding moments of inertia; c_d and k_d are the shaft stiffness and damping constant for the 1st distortion mode with natural

rate in realistic wind conditions is constrained by the allowed level of (harmonic) control effort and stability requirements. The nodding gain K_{nd} is scheduled in a similar way as the PD-gains for the rotational speed error.

Control tool modules. The feedback structures listed above have been implemented in MATLAB program modules for time domain simulation: the MATLAB edition of the control algorithms. The algorithms are also available in the programming languages C and Fortran for straightforward incorporation in process computers and aerodynamic codes.

Besides, interactive program modules have been developed for parametrising the filters and gains of the linear parts in the control loops; these modules include the linearised wind turbine system dynamics. For overall stability and robustness assessment, program modules have been developed for Nyquist analyses of the open loop transfer function. This transfer function is obtained by linearisation of the integrated model of the control loops and the wind turbine, with the main feedback path cut through, that is to say the rotational speed measurement feedback path to the PD-action.

4. SIMULATION RESULTS

The results plotted below apply to a typical multi-MW (off-shore) wind turbine. They have been obtained from the simulation stage in the design tool. Validation runs with the aerodynamic computer code PHATAS [5] (control algorithm included) yielded equal behaviour.

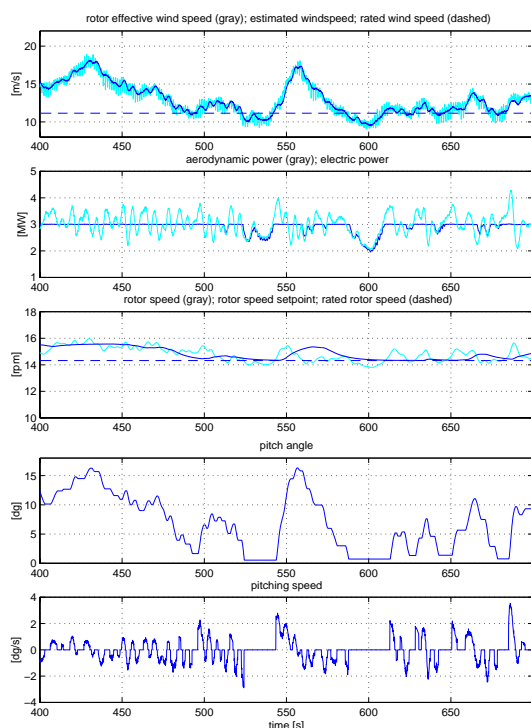


Figure 5: Aerodynamic and electric power control with wind speed estimator

5. CONCLUSIONS

A design tool has been developed for control algorithms for variable speed wind turbines. The by nature multivariable control problem is split-up into physically interpretable control loops that are individually parametrised. These loops pertain to aerodynamic and electric power control and to

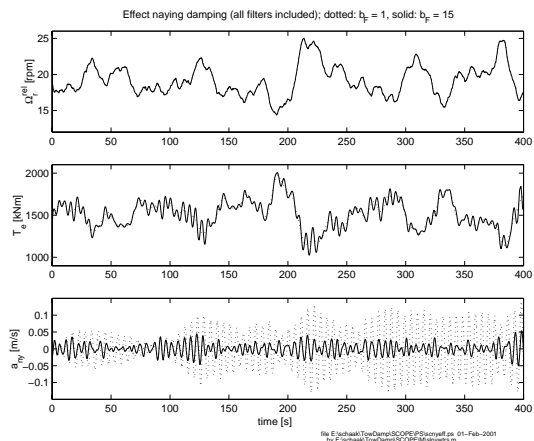


Figure 6: Lateral tower resonance at waves perpendicular to the wind (lower graph: naying acceleration $[m/s^2]$; dash: without damping)

damping of tower bending and drive-train distortion. Special features are (i) dedicated filter design, (ii) wind speed estimation in power control and (iii) shaft distortion estimation by Kalman filtering.

The algorithms with the implemented control loops are clear in implementation and operation, and are on-site tunable by well-educated operators. The C- or Fortran-coded algorithms can be incorporated in process computers and aerodynamic codes with very minor effort.

The approach as implemented in the tool has been extensively validated by non-linear time domain simulations with the authorised aerodynamic code PHATAS [5].

ACKNOWLEDGEMENT

Koert Lindenburg (ECN) is acknowledged for his contribution to dealing with the impact of dynamic inflow on power control and for the many validation runs with PHATAS. Jan Pierik (ECN) is acknowledged for his contributions to electric system modelling and desk top publishing.

REFERENCES

- [1] P.M.M. Bongers; *Modeling and Identification of flexible wind Turbines and a Factorizational Approach to Robust Control*, PhD thesis, ISBN 90-370-0100-9, Delft University of Technology, fac. of Mech. Eng., the Netherlands, 1994.
- [2] S.K. Chakrabarti; *Hydrodynamics of Offshore Structures*, Computational Mechanics Publications Southampton, 1987.
- [3] J.B. Dragt; *Atmospheric Turbulence Characteristics in the Rotating Frame of Reference of a WECS Rotor*. Pp 274-278 in proc. ECWEC Conf. Madrid, Spain, 1990.
- [4] T.G. van Engelen, E.L. van der Hooft and P. Schaak; *Ontwerpgereedschappen voor de Regeling van Windturbines* (in Dutch), Technical report, ECN Wind Energy, Petten, the Netherlands, *Draft*, June, 2001.
- [5] C. Lindenburg and J.G. Schepers; *PHATAS-IV Aeroelastic Modelling, Program for Horizontal Axis Wind turbine Analysis and Simulation, version IV*, ECN Wind Energy, Petten, the Netherlands.
- [6] H. Snel, J.G. Schepers; *Joint Investigation of Dynamic Inflow Effects and Implementation of an Engineering Method*. Technical Report ECN-C-94-107, ECN Wind Energy, Petten, the Netherlands, April, 1995.
- [7] J.F. Wilson; *Dynamics of Offshore Structures*. John Wiley & Sons, 1984.